METEORITICS & PLANETARY SCIENCE

Noble gases and nitrogen in the Almahata Sitta ureilite

Journal:	*Meteoritics & Planetary Science*
Manuscript ID:	MAPS-1282.R2
Manuscript Type:	Article
Date Submitted by the Author:	n/a
Complete List of Authors:	Sripada, Murty; Physical Research Laboratory, Planetary and Geosciences Division Mahajan, Ramakant; Physical Research Laboratory, Planetary Sciences Division Jenniskens, Peter; SETI Institute Shaddad, Muawia; University of Khartoum, Dept. of Physics Eldien, Beder; University of Khartoum, Dept. of Physics
Keywords:	Meteorite(s), Nitrogen, Noble Gases, Ureilites

Noble gases and nitrogen in the Almahata Sitta ureilite

S. V. S. Murty[1*], R. R. Mahajan[1], Peter Jenniskens[2], Muawia H. Shaddad[3], and Beder Eldien[3]

(1) Planetary and Geosciences Division, Physical Research Laboratory, Ahmedabad 380 009, India

(2) SETI Institute, Carl Sagan Center, 515 North Whisman Road, Mountain View, California 94043 USA

(3) University of Khartoum, Department of Physics, P. O. Box 321, Khartoum 11115, Sudan

Submitted to *Meteoritics and Planetary Science*: January 2010

3 Tables

9 Figures

Keywords: Noble gases, Nitrogen, Ureilites, Meteorites, Almahata Sitta meteorite

Suggested Running Title: Noble Gases and Nitrogen in Almahata Sitta

*Corresponding author: murty@prl.res.in

ABSTRACT

A bulk sample (split from Almahata Sitta #36) and an acid resistant residue (from #44) have been analysed for noble gases and nitrogen by step-wise combustion/pyrolysis. In the bulk sample, He and Ne are a mixture of cosmogenic and trapped components. Cosmic ray exposure ages of 13.8 and 16.0 Ma are calculated based on ^{3}He and ^{21}Ne respectively. Except for a small amount of cosmogenic ^{3}He, He and Ne in the acid resistant residue are not significantly above blank level. Ar, Kr and Xe in both the bulk and residue are dominated by a trapped component, but the elemental ratios are different. While the ratios of ^{36}Ar/^{132}Xe and ^{84}Kr/^{132}Xe are about 400 and 1, respectively, in all the combustion steps of the residue, the bulk sample has about an order of magnitude more ^{132}Xe in the corresponding combustion steps. It seems, an acid soluble phase is the host of this Xe-rich carrier and is different from a similar phase observed in the ureilite ALH 82130. Nitrogen in the bulk sample and acid residue are 21.1 ppm (-36.8‰), and 249.5 ppm (-74.3‰), respectively. Peak release of C (monitored as CO + CO_2), N, Ar, Kr and Xe occurred at the 700^{o}C combustion step of the residue, confirming diamond as the principal carrier for these gases. In the residue, the isotopic ratio ^{38}Ar/^{36}Ar shows a monotonic increase with release temperature.

1. INTRODUCTION

Ureilites are the second largest group of achondrites in our collection (Mittlefehldt et al., 1998), although the number of observed falls is only 7. Almahata Sitta (hereafter AS) is the most recently fallen ureilite, the least weathered in our collection, and is classified as an anomalous polymict ureilite, anomalous on account of some collected fragments being rich in pores (up to 20%) and carbonaceous matter

(Jenniskens et al., 2009). It is the first meteorite to be associated with a known small asteroid of size ~4 m, called 2008 TC_3, predicted and observed to hit the earth on Oct. 7, 2008 in the Nubian Desert of Sudan (Yeomans, 2008; Jenniskens et al., 2009; Borovicka and Charvat, 2009). AS has three major lithologies that are not homogeneously distributed at gram sample level, with several clasts found scattered among these lithologies (Zolensky et al., 2010).

Ureilites are enigmatic meteorites showing both primitive and igneous characteristics. Heterogeneous oxygen isotopic composition, falling along the CCAM line in the three isotope plot (Clayton and Mayeda, 1988), occurrence of large amounts of trapped noble gases, mostly hosted in elemental C (Göbel et al., 1978; Rai et al., 2003a) and coexistence of multiple nitrogen components (Yamamoto et al., 1998; Rai et al., 2003b) are some of the primitive features, while the mineralogy, texture and chemistry suggest them to be highly fractionated rocks (Goodrich, 1992; Mittelefehldt et al., 1998). Though the carrier of trapped noble gases is shown to be elemental C , mostly diamond (Göbel et al., 1978; Rai et al., 2003a) or amorphous C, in case of ALH 78019 (Wacker, 1986; Rai et al., 2002), there are some suggestions that graphite is a likely candidate as well (Okazaki et al., 2003). Earlier work has identified the typical elemental and isotopic ratios of N, N/C and $N/^{36}Ar$ in the host phases of monomict and polymict ureilites (see Table 5 in Rai et al., 2003b).

Different models have been proposed for the formation of ureilites that describe them as multi-stage igneous cumulates (Berkley et al., 1976, Berkley, 1989; Goodrich et al., 1987), residual partial melts (Boynton et al., 1976; Spitz and Boynton, 1991; Scott et al., 1993; Wasson et al., 1976), collision products of primitive planetesimals (Takeda, 1987; Takeda et al., 1989; Warren and Kallemeyn, 1989) and a result of smelting of an olivine rich parent body (Singletary and Grove, 2003; Walker and

Grove, 1993; Warren and Kallemeyn, 1992). Early smelting or partial melting events suggested by Hf-W systematics may prevent the homogenisation of the primitive features like oxygen isotopic composition and the presence of primordial noble gases in the ureilite parent body (Lee et al., 2009).

The fresh nature of Almahata Sitta, the corroborating information about the size of the asteroid prior to impact, and the unusual properties of this meteorite make it an interesting case to study the volatiles nitrogen and noble gases.

2. SAMPLE PREPARATION

As part of a consortium study, we received two fragments from samples #44 and #36. Sample #36 is from a 58 g meteorite found at Long. = 32.51850º and Lat. = +20.71195º, with a density of 2.67 g/cc, while sample #44 consisted of small fragments (possibly broken from a larger fallen meteorite during impact) lying in the sand at Long. = 32.49690º and Lat. = +20.70178º, with total weight of 2.3 g. Our bulk sample is from #36 and hence is a fresh interior chip.

We have dissolved the piece from #44 (178.4 mg) to obtain acid resistant residue, with the hope that any adhering terrestrial material will dissolve in acids and does not contribute to the noble gases. The HF/HCl acid residue is prepared by the procedure described earlier (Rai et al., 2003b). Briefly, the finely powdered sample is treated alternately with 10N HF/6N HCl and 6N HCl. This procedure was repeated 6 times. The residue was then washed with water under ultrasonication, several times, until the pH becomes neutral. After subsequent washes with alcohol and acetone, the residue is air dried. The yield at this stage is ~7 mg (about 4% of starting mass, and is in the range observed for most ureilites, Rai et al., 2003a). Residues from ureilites, produced

by the same procedure by earlier workers, have shown them to be mostly C phases (Göbel et al., 1978; Ott et al., 1984).

For the residue we have only investigated the morphological features by SEM and took EDX spectra to qualitatively identify the major elements. In most grains only a C line is seen. Fig. 1 gives the SEM pictures of the residue. The residue is mostly made of crystallites of graphite (dark grey in colour) of ~10 microns, with coatings of amorphous C. In addition, whitish crystals of diamond, few microns to sub micron size are also in abundance. The amorphous C phase, seen as coating on graphite crystals, seems to be a minor phase.

The bulk sample (as received) and the residue have been packed into gold foil (to enable combustion up to 1030^{o}C) and loaded into the noble gas extraction system. The samples are degassed overnight under vacuum at 150^{o}C, with an infra red lamp, to drive off the adsorbed gases. After obtaining satisfactory system blanks, the sample analysis has been started.

Experimental

The bulk samples were combusted under 2 Torr O_2 pressure at the following temperatures (in ^{o}C, 300, 400, 600, 800 and 1000) before pyrolysing at 1200, 1400 and 1800^{o}C in a Mo crucible. The acid residue was only combusted at 300, 400, 450, 500, 600, 700, 800 and 1030^{o}C. For combustion, O_2 was generated from Cu/CuO finger, until the required pressure is reached in the sample chamber, a double walled quartz finger, with outer layer of secondary vacuum. The sample is kept at the desired temperature for 45 minutes, after isolating the Cu/CuO finger. At the end of the combustion, the remaining O_2 has been removed by exposing to Cu/CuO finger at 400^{o}C. At this stage, about 10% of extracted gas has been isolated for later processing for N_2 analysis and the rest is cleaned on Ti/Zr and Ti/Pd getters to remove active

gases. The heavy noble gases (Ar, Kr and Xe) are held back on a charcoal finger kept at liquid nitrogen temperature, and the He, Ne fraction is admitted into the mass spectrometer (VG1200, MicroMass) for analysis. Subsequently, the Ar, Kr and Xe fraction is admitted into the mass spectrometer. After a quick scan of the peak heights of ^{36}Ar, ^{84}Kr and ^{132}Xe, for abundances, Ar, Xe and Kr are run for isotopic analysis. The procedures have been described in earlier publications (Rai et al., 2003a, b).

Blanks were run under identical conditions of sample analyses. For N and heavy noble gases the blank contribution is < 5% for all temperature steps. For ^{4}He and Ne, the blank contribution is <15% for the bulk sample, but for the residue sample, blank contribution is up to 50% at some temperatures,(≥600^{o}C) making the isotopic ratios susceptible to blank correction, though the signals at ^{4}He and ^{22}Ne allowed estimation of their abundances. Hence we only report ^{4}He and ^{22}Ne amounts for the residue sample. ^{3}He on the other hand has a negligible blank, making it possible to detect even small amounts with ease.

Air standards were analysed to ascertain the sensitivity and mass discrimination corrections. The data reported has been corrected for blanks, mass discrimination and interferences from CO_2^{++} (^{22}Ne), $^{40}Ar^{++}$ (^{20}Ne) and CO (N_2) as detailed earlier (Murty, 1997; Rai et al., 2003a, b). In our earlier work on the measurement of Ar isotopic composition in ureilites, we have identified a pressure dependence on the mass discrimination on the $^{38}Ar/^{36}Ar$ ratio and have worked out the correction factor to take this into account (Rai et al., 2003a). The Ar isotopic data presented here has been corrected for the pressure dependant mass discrimination, as detailed in Rai et al., (2003a).

3. RESULTS

The data of all noble gases for the totals of the bulk sample and acid residue are given in Table 1. N data, cosmogenic He, Ne, production rates and exposure ages are listed in Table 2. Table 3 gives the individual temperature data, for both bulk and acid residue.

He and Ne

For the bulk sample, He, Ne isotopic ratios clearly indicate that they are a mixture of trapped and cosmogenic components. Cosmogenic ^{3}He has been estimated by assuming radiogenic ^{4}He to be negligible, because the U content in ureilites is ~ 1 ppb (Higuchi et, al., 1976), and taking $(^{3}He/^{4}He)_{t} = 1.4x10^{-4}$ and $(^{3}He/^{4}He)_{c} = 0.2$. We calculated $^{3}He_{c}$ (in units of 10^{-8} ccSTP/g) of 23.2 and 12.6 for the bulk and acid residue respectively.

Ne three isotope plot for the temperature steps of the bulk sample (Fig. 2) fall along the mixing line between cosmogenic and a trapped component (Ne-U). There is no solar Ne in AS as observed in some polymict ureilites (Ott et al., 1993). We calculated the cosmogenic ratio $(^{22}Ne/^{21}Ne)_{c} = 1.063\pm0.017$, by taking the trapped composition as Ne-U [$^{20}Ne/^{22}Ne = 10.4\pm0.3$ and $^{21}Ne/^{22}Ne = 0.030\pm0.005$, Ott et al. 1985] and estimated the $^{21}Ne_{c} = 9.08x10^{-8}$ ccSTP/g (listed in Table 2).

For the calculation of production rates, we have used the average chemical composition of ureilites (arithematic mean of six ureilites, as listed in Vdovykin, 1976) [in wt. %, Mg = 21.81; Al = 0.25; Si = 18.6; S = 0.33; Ca = 0.71; Fe = 14.62; Cr = 0.508; Ti = 0.07; Mn = 0.29; Ni = 0.131]. We derived the production rates based on the empirical equation of Eugster and Michel (1995) for diogenites and for shielding

depth indicated by the ratio $(^{22}Ne/^{21}Ne)_c = 1.063$. The production rates [in units of 10^{-8} ccSTP/g/Ma] obtained by us ($P_3 = 1.68$; $P_{21} = 0.567$) and the exposure ages derived ($T_3 = 13.8$ Ma; $T_{21} = 16.0$ Ma) are in the range of values reported by Welten et al., 2010 and Ott et al., 2010, within the uncertainities of ±15%. Exposure ages of ureilites span a range of values, with a low value of 0.1 Ma for ALH78019 to a high value of 46.8 Ma for EET83309, with no appreciable age clustering (Rai et al., 2003a, Aylmer et al., 1990). Exposure age of 16 Ma for AS is thus normal for an ureilite.

^{3}He is mostly cosmogenic in AS. Release patterns of ^{3}He and $CO+CO_2$ are shown in Fig. 3 for both the bulk sample and the acid residue. ^{3}He has a bimodal release in both cases. The main target element for ^{3}He is pure carbon for the residue and the peaks at 600°C and 1030°C combustion steps correspond to diamond and coarse grained graphite. Assuming quantitative retention of ^{3}He by both these phases, one can infer about equal proportion of diamond and graphite in the acid residue. The C release in the temperature intervals 500-700°C and 800-1030°C, where diamond and graphite usually combust (Rai et al., 2003a) further support this inference. Confocal Raman imaging spectroscopy has shown that the major C phase in AS is highly crystalline graphite (Ross et al., 2010). Amorphous carbon combusts below <500°C, wherein negligible pressure of $CO + CO_2$ has been observed, suggesting that amorphous C is a minor phase in the residue. For the bulk sample, on the other hand, target elements for ^{3}He are not limited to C. The low temperature peak of ^{3}He could be mostly contributed by C phases while the high temperature release could be due to a mixture of C (protected in metal/silicate phases) and other phases like metal/silicate.

Ar, Kr and Xe

The data for the totals of Ar, Kr and Xe are given in Table 1. The isotopic composition of Kr and Xe is similar in all temperature steps for both bulk and residue samples and grossly matches that of Kenna (Wilkening and Marti, 1976) and will not be discussed in this paper. The $^{38}Ar/^{36}Ar$ ratio for the total of the residue matches with the average ureilite value of 0.190 ± 0.001, derived from the values of acid residues of seven ureilites from Göbel et al. (1978). The higher value of $^{38}Ar/^{36}Ar$ of 0.1954 for the bulk sample is due to the cosmogenic Ar. Due to the large amount of trapped Ar (compared to cosmogenic Ar) even in the bulk sample, deriving the cosmogenic ^{38}Ar will have a lot of uncertainty, so we do not use cosmogenic ^{38}Ar for estimating the cosmic ray exposure age of AS. The $^{40}Ar/^{36}Ar$ ratios of the bulk and residue are 6.8 and 0.2, while the lowest values measured are 2.4 (in 1400°C Pyrolysis) and 0.14 (700°C combustion) in the bulk and residue respectively. The higher values in the bulk are due to the in situ produced radiogenic ^{40}Ar from ^{40}K decay. Compared to the lowest $^{40}Ar/^{36}Ar$ value of (2.9 ± 1.7) x 10^{-4} in the acid residue of Dayalpur (Göbel et al., 1978), the value for AS is high, even though the trapped Ar amount is very high. This may indicate either the presence of air contamination, K content in acid residue or the presence of a K carrying phase that tagged along with C phases. But the elemental ratios of noble gases clearly rule out air contamination as the possible cause.

Nitrogen

Nitrogen data for the totals is given in Table 2 and for the individual temperature steps is compiled in Table 3. N release pattern, along with the C release (monitored as CO + CO_2) for the bulk and the residue are shown in Fig. 4. The bulk sample has 21.1 ppm N with $\delta^{15}N$ of -36.8‰, with a peak release at 1000°C, which also shows the lightest N composition (-94.3‰). Isotopic composition of N up to 600°C has a

signature of ~ +30‰, then reaches a minimum of -94.3‰ at 1000°C and in subsequent steps shows an excursion between -20 and -69.4‰. The HF/HCl residue has an N content of 249.5 ppm with a composition of -74.3‰. There is a minor peak at 400°C with +12‰, and a major release at 700°C (-115‰) and about 26% N is released in the subsequent combustion steps at 800 and 1030°C.

4. DISCUSSION

Cosmic ray exposure age

The agreement, within experimental uncertainties, between the exposure ages based on ^{3}He and ^{21}Ne suggests no ^{3}He loss in #36. Also, our value of T_{21} = 16.0±2.4 Ma for AS#36 is in agreement with the value of 14.1 Ma, as well as the average exposure age of 15±2 Ma, from the four fragments #4, #36, #44 and #47 (Welten et al., 2010). The Bern plot of Welten et al.,2010, also does not indicate any ^{3}He loss, though, partial loss of ^{3}He is indicated for #1 (Ott et al., 2010). Of the five fragments of AS (1, 4, 36, 44 and 47) for which exposure ages are determined, fragments #1 and #44 are from shallower depth, while #47 is more deeply shielded (based on their $(^{22}Ne/^{21}Ne)_c$ ratios). Considering that the size of AS has been estimated to be ~4 m in diameter, no complex exposure is indicated. It is surprising that a ~4 m object with a porosity of up to 55% survived for 16 Ma since breakup from its parent asteroid till fall on earth.

Trapped gases

One of the features of ureilites is the presence of large concentrations of trapped noble gases, and a principle N component with an isotopic signature of ~ -100‰, hosted in diamonds (Göbel et al., 1978; Rai et al., 2003a,b). Additional N components have also been identified in the carriers amorphous carbon and graphite (Rai et al., 2003b) while it has been demonstrated that graphite is devoid of noble gases (Wacker

1986, Rai et al., 2002), although amorphous C may contain noble gases in some ureilites (Wacker 1986; Rai et al., 2002, 2003a). Noble gas abundances and release patterns in the ureilite AS show some feature not observed earlier and hold clues to the noble gas carriers and gas trapping process(es).

Release pattern of C phases has been monitored during combustion as pressure of $CO + CO_2$ by the Convectron pressure gauge. During the subsequent pyrolysis of the bulk sample, there is also release of $CO + CO_2$, due to oxidation of C that is entrapped within silicates, by the solid state reaction with the oxygen from silicates. In Fig. 5 the release patterns of C, N, Ar, Kr and Xe from the acid residue for AS have been compared with those of typical monomict, polymict and diamond free ureilites and from the most reduced and low shocked ALH 82130 having unusual noble gas elemental ratios, $^{36}Ar/^{132}Xe$ ~ 19 and 13 for bulk sample and HF/HCl residue, as against the average values of ~ 100 and ~ 200 respectively (Rai et al., 2003a). A sharp release of N, Ar, Kr and Xe, at the same temperature as peak C release also occurs is seen for the typical monomict (LEW 85328) and polymict (EET 87720) ureilites. ALH 78019 has peak release (~90%) of noble gases and ~50% N at 400°C (wherein negligible amount of C is released), while most C release occurs at > 600°C, with negligible amount of noble gases, but ~ 40% N. Studies of ALH 78019 have given a clear indication that its major C phase (crystalline graphite) contains no detectable noble gases and the minor C phase (amorphous carbon) is the principal noble gas carrier (Rai et al., 2002). The C release pattern of AS residue shows about 50% release in the 500-700°C interval and the remaining 50% combusting at 800-1030°C steps and carrying ~40% of Ar, Kr, Xe and ~25% N in the later two steps. AS release pattern has features that partly resemble those from ALH 78019, EET 87720 and other monomict ureilites.

Elemental ratios

The elemental ratios of trapped noble gases in ureilites span a considerable range of values for $^{132}Xe/^{36}Ar$ and $^{84}Kr/^{36}Ar$, but in a plot of $^{132}Xe/^{36}Ar$ Vs. $^{84}Kr/^{36}Ar$ they mostly plot along the mass fractionation line, with very few exceptions, such as in the cases of ALH 82130 and EET 83309 (Rai et al., 2003a; Ott et al., 1993), indicative of a relative enrichment of ^{132}Xe in these two urilites. In Fig. 6, the ratios of $^{36}Ar/^{132}Xe$ and $^{84}Kr/^{132}Xe$ for different temperature fractions of AS bulk and residue have been compared. For the AS residue, the $^{36}Ar/^{132}Xe$ ratios fall within the average ureilite range and the $^{84}Kr/^{132}Xe$ ratios also match the average ureilites range within a factor of two. For the AS bulk sample, on the other hand, both the ratios $^{36}Ar/^{132}Xe$ and $^{84}Kr/^{132}Xe$ are lower by factors of about 10 and 5 respectively, relative to the average, indicating enrichment of heavier noble gases. The elemental ratios for the totals of AS-Bulk and AS-Residue are plotted in Fig. 7, wherein the mass fractionation line (mfl), along which most of the data of bulk and acid residues of ureilites fall (see Fig. 12, Rai et al., 2003a), is also shown. While the point AS-Bulk falls above the mfl, the point AS-Residue falls along the line. The deviation of AS-Bulk from mfl can be explained by enrichment of ^{132}Xe. Similar Xe enrichment has been observed in the monomict ureilite ALH82130 (bulk and acid residue) and polymict ureilite EET83309. Data for both these ureilites are also shown in Fig.7. The different features in the bulk and residue samples suggest the loss of a phase during acid dissolution from the bulk sample, where heavier noble gases are enriched. A similar feature has been observed in the bulk samples of ALH 82130 (monomict) and EET 83309 (polymict) (Rai et al., 2003a; Ott et al., 1993), but there are differences in the acid resistance of the heavy noble gases enriched phase(s) as well as in enrichments in these three ureilites. ALH

82130 has only Xe enrichment in the bulk which survived the HF/HCl treatment and to some extent, even after treatment with $HClO_4$ (Rai et al., 2003a). EET 83309 showed enrichments in both ^{84}Kr and ^{132}Xe, which survived the HF/HCl treatment, but on further treatment with HNO_3, the Xe enrichment vanished and the ^{84}Kr enrichment still survived.

Another important difference in these three cases is in the variation of the elemental ratios with temperature. There is a general increase of the ratios $^{36}Ar/^{132}Xe$ and $^{36}Ar/^{84}Kr$ with extraction temperature, during combustion release from C rich residues for ALH 82130 and EET 83309 (Rai et al., 2003a), whereas the ratios are remarkably uniform at all temperatures, in the case of AS residue (See Fig. 6). This clearly suggests the presence of at least two different carrier phases for noble gases in AS, one is an HF/HCl resistant C phase having the elemental ratios similar to the average values found among other ureilites, while the other phase is either acid soluble or lost as a colloid during the process of preparing the residue, and having relatively higher (by an order of magnitude) Xe. It is possible that the Xe enrichment is a result of partial loss of Ar and Kr, from a labile phase in a heating event. This could have happened in the breakup event leading to the ejection of AS meteoroid from the parent asteroid.

Nitrogen components and carriers

The bulk sample shows at least three isotopic components (see Fig. 4). A component with $\delta^{15}N$ of 31.8‰ released in the low temperature (300 to 600°C) interval, a lighter N component having <-94‰, with peak release at 1000°C and an admixture of this light component with a component heavier than -20‰ in the temperature fractions 1200 to 1800°C. The slightly lower $\delta^{15}N$ values for the 300°C

and 600°C fractions (as compared to the 400°C fraction is due to a small amount of adsorbed air and a small release of the more tightly bound lighter N respectively. Such heavy N has been observed in other ureilites as well (Rai et al., 2003b) and has been identified with amorphous C, having a lower combustion temperature (Rai et al., 2002). The peak release at the 1000°C combustion, with the lightest composition is due to the diamond, which has a $\delta^{15}N$ of -115‰, as observed in both monomict and polymict ureilites (Rai et a., 2003b). In the subsequent pyrolysis steps, the diamonds that are protected inside silicates and metal and hence not accessible to the external oxygen, and another metal/silicate phase, carrying N with $\delta^{15}N \geq$-20‰ are co-released, resulting in the excursions in the observed N isotopic structure. This metal/silicate phase with $\delta^{15}N \geq$-20‰ could be the clast material observed in AS (Zolensky et al., 2010) and other polymict ureilites (Mittelfehldt et al., 1998) and attributed as the possible carrier of heavy N in polymict ureilites (Grady and Pillenger, 1988).

The N release from the HF/HCl residue is bimodal with a minor peak at 400°C (with $\delta^{15}N$ ~12‰) and a major peak at 700°C (with $\delta^{15}N$ ~115‰). Slightly lower $\delta^{15}N$ values in the 300°C and 450 and 500°C fractions, as compared to the +12‰ value in the 400°C fraction are due to a small amount of adsorbed air in the 300°C fraction and a small release of light N in the 450 and 500°C fractions respectively. Though both bulk and residue samples show light N with -115‰ as a major N component, consistent with the expected combustion/pyrolysis steps for diamond to be the carrier, the low temperature steps in bulk and residue show heavy $\delta^{15}N$ that differ by ~20‰. This can not be attributed to air contamination in the low temperature (LT) steps of residue, as the corresponding $^{40}Ar/^{36}Ar$ ratios are ≤1. The N/C ratios of the LT fractions ($\leq 3 \times 10^{-3}$) rule out organic contamination during sample preparation. The N/C of the 300 to 600°C fractions of the bulk sample is 0.0456 (assuming 4% C

in the analysed sample). If the LT N release in the residue is also represented in the bulk, an additional non-carbonaceous, acid soluble N phase with $\delta^{15}N>30‰$ is needed in the bulk sample. The elemental ratio $N/^{36}Ar$ in the LT of residue and bulk are 7×10^3 and 588×10^3 respectively, clearly indicating the possibility of a non-carbonaceous N carrier, considering the fact that most trapped noble gases are hosted by C phases. The numerous clasts observed in all three major lithologies of AS (Zolensky et al., 2010) could be the host phase of this heavy N carrier.

Argon isotopic variations

Argon in the residue is purely of trapped origin for the isotopes ^{36}Ar and ^{38}Ar, while ^{40}Ar could have a small radiogenic contribution, depending on the K abundance. The isotopic ratio $^{38}Ar/^{36}Ar$ is expected to be representative of the trapped component only, except for fractionation effects due to possible loss processes or acquisition mechanism. The ratio for the total of the residue 0.1908 ± 0.0002 matches with the average value for ureilites residues 0.190 ± 0.001 (average value of seven ureilite residues, taken from Göbel et al., 1978). However, the ratios for the temperature steps show a monotonic increase from 0.1890 (in 300°C fraction) up to 0.1916 (in 1030°C fraction). Fig. 8 shows the trend of $^{38}Ar/^{36}Ar$ ratio against release temperature. There is almost a linear increase of the isotopic ratio with temperature. Though the total value falls within the average ureilites range, the values at high temperatures clearly are above this range. It is possible that the observed trend is an artefact of the correction employed for the pressure dependence on the $^{38}Ar/^{36}Ar$ ratio observed in our earlier work (Ra et al., 2003a), but this can be ruled out by the following observation. In the same plot, the ^{36}Ar amount (the most abundant isotope in the ureilite Ar) in each temperature fraction is also shown. The peak amount of ^{36}Ar and

the peak value of $^{38}Ar/^{36}Ar$ do not show a parallel. If the observed variation in the $^{38}Ar/^{36}Ar$ ratio is a consequence of the pressure of Ar in the mass spectrometer, a parallel behaviour is expected, safely ruling out the pressure effect as the plausible cause of this variation. Also, our earlier observation is a lowering of the $^{38}Ar/^{36}Ar$ ratio as the pressure of Ar increases and not as observed in the release pattern.

This isotopic variation can be due to two possible reasons related to either release process or due to incorporation process. The observed isotopic change could be due to diffusive fractionation from a uniform reservoir, with progressive enrichment in the heavy isotope at higher temperature fraction that is released later. However, a very low diffusion coefficient for diamond (Ozima, 1989; Göbel et al., 1978), the principal noble gas carrier, at the temperatures of interest rules out this possibility. An increase of the elemental ratios $^{36}Ar/^{132}Xe$ and $^{36}Ar/^{84}Kr$ as the temperature of combustion increases has been interpreted as due to noble gas incorporation into diamonds by ion implantation (Rai et al., 2003a). This process, resulting in a change of the elemental ratios by more than an order of magnitude is expected to result in a measurable change in isotopic ratio of at least the lighter element Ar. The isotopic changes in the $^{38}Ar/^{36}Ar$ ratios observed in AS residue will be in accordance with the expectation of heavy Ar isotope enrichment. But the magnitude of change (1.37%) in the Ar isotopic ratio is expected to result in an elemental ratio change of more than two orders of magnitude in $^{36}Ar/^{132}Xe$, while the observed elemental ratios (335-448) are surprisingly very uniform (within 30%) in all temperature fractions. The above two possibilities can hence be ruled out.

The observed variations could be due to a two component mixing, where two reservoirs of trapped Argon are present with normal (average ureilite composition) and with higher $^{38}Ar/^{36}Ar$ ratio, the latter being sited in the phase with high

temperature (HT) release. Fig. 9 is a plot of $^{38}Ar/^{36}Ar$ versus the corresponding $\delta^{15}N$ for the temperature steps of residue sample. The data shown in Fig. 9 fall into two clusters. One of the clusters corresponds to LT fractions with normal $^{38}Ar/^{36}Ar$ and heavy $\delta^{15}N$ and the second one with higher $^{38}Ar/^{36}Ar$ and light $\delta^{15}N$. As already discussed we can use the N compositions to identify the LT and HT phases as amorphous C and diamond respectively. The question then is why Ar composition is enriched in the HT (diamond) component, while the $\delta^{15}N$ agrees with the composition found for diamonds in other ureilites.

Noble gas carriers

Earlier work has shown that the principal noble gas carriers in ureilites are amorphous C and diamond (Göbel et al., 1978; Wacker, 1986; Rai et al., 2003a), while graphite is devoid of noble gases (Rai et al., 2002). An additional noble gas carrier, probably kamacite has been suspected (Göbel et al., 1978). There have been hints of graphite being a noble gas carrier in ALH 78019 (Okazaki et al., 2003). The largest concentration of noble gases has so far been observed in the Dayalpur residue B-2-1, at 78.3 x 10^{-5} ccSTP^{36}Ar/g (Göbel et al., 1978). The AS residue with a ^{36}Ar amount of 45.3 x 10^{-5} ccSTP/g ranks second, among the data available on ureilites. Compared to the bulk sample of AS (represented here by fragment #36), the residue is enriched by factors of 1043, 529 and 119 respectively in trapped ^{36}Ar, ^{84}Kr and ^{132}Xe. This non-uniform enrichment is due to the presence of a phase in the bulk sample (of AS#44) with enrichments in ^{84}Kr and ^{132}Xe, compared to the residue. We did not measure the bulk sample AS#44. Welten et al., 2010 have reported ^{36}Ar amount (in ccSTP/g units) in both AS#36 ($13.1x10^{-8}$) and AS#44($1390x10^{-8}$), and they differ by about a factor of 100. Our value of ^{36}Ar in AS#36 is high by a factor of 3.3, compared to Welten et al.,

2010 value.. Further, the reported concentrations of Ar, Kr and Xe in AS#1 and AS#47 also show a facot of 5 variation (Ott et al., 2010). These variations are due to the heterogeneous distribution of the carrier phases of trapped noble gases in the few milligrams range of sample sizes being analysed. Ar, Kr and Xe are dominated by trapped component and mainly carried by the diamond phase, as indicated by the co-release of C, Ar, Kr and Xe at the 700°C combustion step of the residue and the accompanying $\delta^{15}N$ (see Fig. 4). But about 40% C release along with the accompanied noble gases has occurred in the 800 and 1030°C combustion steps for the residue (see Fig. 4). While most of the C release in these later two steps is likely contributed by the noble gas poor coarse grained graphite (see SEM pictures of residue in Fig. 1), (Rai et al., 2002), the noble gases must have been contributed by the coarse (~µm) sized diamonds which combust at higher temperature. The oxygen made available during combustion is enough to completely oxidise the total C in the sample. Hence, the combustion reaction is not O_2 limited. Rather, it is reaction rate limited, due to the fact that coarser diamond takes longer time to get oxidised due to the smaller surface area. This results in the release of gases from coarser diamonds in higher temperature combustions. The accompanying $\delta^{15}N$, with typical -115‰ signature of diamonds further affirms the diamond origin for the noble gases released in the 800°C and 1030°C fractions. SEM pictures of the residue clearly show large graphite crystals (dark grey crystals showing layering) and more than one size range of much smaller diamond crystals (whitish colored crystals) and both these phases have been coated with amorphous C. The coarse grained graphite might be combusting at >700°C, and hence may overlap with the region where the coarse diamonds (around a few microns in size) are combusting and releasing their trapped noble gases and nitrogen, explaining the continued release of N and Ar, Kr, Xe at

800°C and 1030°C combustion steps. Diamond aggregates ranging upto several micrometers in dimension, contained within graphite grains have been identified by confocal Raman imaging spectroscopy (Zolensky et al., 2010). Though it is not possible to estimate the relative proportions of graphite and the diamond aggregates (of several microns size) contained within the graphite, visual indications from SEM pictures suggest graphite to be the predominat C phase combusting in the 800-1030°C interval. As graphite is gas poor, to account for the ~40% release of Ar, Kr, Xe by the coarse sized diamonds necessarily implies a larger concentration of noble gases in the coarse diamonds (as compared to the sub-micron diamonds, predominantly releasing their gases in the 600-700°C combustion steps.

Noble gas trapping mechanism

Ureilite noble gases are highly fractionated in favour of heavy elements with respect to the solar component. Despite orders of magnitude variations in the absolute amounts in several ureilites, their isotopic composition is similar (Göbel et al., 1978; Rai et al., 2003a) and closely matches with 'Q component' (Busemann et al., 2000). Amorphous carbon and diamond have been shown to be the carrier phases of noble gases in ureilites. The possible trapping mechanisms into these C phases to produce the observed elemental pattern have been thoroughly discussed in literature (Rai et al., 2003a and references therein) and will not be repeated here. Rayleigh distillation (Ozima et al., 1998), solubility or physical adsorption (Wacker, 1989), and ion implantation from nebular plasma (Göbel et al., 1978; Matsuda et al., 1991; Matsuda and Yoshida, 2001; Rai et al., 2003a) are the processes considered. Rai et al. (2003a) have favored the ion implantation mechanism from nebular plasma based on the observed change in the elemental ratios $^{132}Xe/^{36}Ar$ and $^{84}Kr/^{36}Ar$ with depth in the diamond grains and its match with the ion implantation simulation (Ziegler et al.,

1985). Artificial ion implantation experiments into synthetic nano-diamonds also favoured this mechanism for gas acquisition by presolar diamonds (Koscheev et al., 2001). The uniform elemental ratios at all combustion steps for the AS residue and the variation of the isotopic ratio $^{38}Ar/^{36}Ar$ require a different mechanism or a subsequent alteration to explain these observations. The elemental and isotopic ratios of heavy noble gases in AS may hold clues in providing information on the noble gas trapping in C phases of ureilites, but more work is needed to decipher this information.

5. CONCLUSIONS

Cosmogenic and trapped noble gases and nitrogen have been investigated in a bulk sample and an acid resistant C rich residue of the anomalous ureilite Almahata Sitta. He and Ne are a mixture of trapped and cosmogenic components. The cosmic ray exposure age based on ^{21}Ne (16 Ma) is in the range of values observed for other ureilites.

The uniform elemental ratios at all combustion temperatures for the residue and the increase in the ratio of $^{38}Ar/^{36}Ar$ are contrary to the expectations of noble gas acquisition by diamonds through ion implantation mechanism from hot plasma (Rai et al., 2003a). Argon isotopic variation can be best explained by a two component mixing, as also indicated by the accompanying N isotope composition. But at present there is no satisfactory mechanism to explanation how Ar becomes enriched in heavy isotope in the component released at high temperature.

Earlier studies have shown the presence of solar Ne in some polymict ureilites (Ott et al., 1993) while trapped Ne in AS is Ne-U. Some polymict ureilites have also been observed to host a heavy N component, with $\delta^{15}N$ up to +600‰ (Grady and

Pillinger, 1988) and also containing an amorphous C phase having $\delta^{15}N \geq 50‰$ and carrying noble gases. Such an amorphous C phase is also missing in AS. The polymict ureilite EET83309 has a C phase (probably a gas bearing graphite or cohenite) carrying noble gases and N with $\delta^{15}N \geq 153‰$, and combusting at <700°C (Rai et al., 2003b). AS does not have this type of C phase either.

Two features found in AS #36 and #44, the uniform elemental ratios in the residue at all release temperatures and the increase in the isotopic ratio $^{38}Ar/^{36}Ar$ with increasing extraction temperature have not been found in any other ureilite. This makes AS a truly anomalous polymict ureilite. Some of these anomalous features could be primary (nebular/parent body related) and some could be due to atmospheric ablation and consequent loss/gain of noble gases. The impact of asteroid 2008 TC_3 was accompanied by three intense detonations at 45-35 km altitude, with meteoric plasma reaching temperatures of ~3,650K (Borovicka and Charvat, 2009). Considering the fact that most of the recovered AS pieces are small (<379 g), and in particular, the residue has been prepared from small fragments (#44), it is possible that some of the results may be partially affected by gas loss/exchange during the fragmentation and fireball flares. Further investigations will be needed to ascertain the primary/ablation causes and their implications to the noble gas incorporation into the C phases of ureilites.

ACKNOWLEDGEMENTS

Suruchi Goel has helped in the preparation of the acid residue. Dipak Panda and Suruchi Goel are thanked for the SEM work. Students and staff of the University of Khartoum collected the meteorites. We thank R. Okazaki and Rainer Wieler for

critical reviews and the AE, A.J.T. Jull for useful comments. Discussions with U. Ott have been helpful in improving the presentation. Murty thanks the Department of Space, Government of India for the financial support. PJ is supported by a NASA Planetary Astronomy grant.

REFERENCES

Aylmer D., Vogt S., Herzog G.F., Klein J., Fink D. and Middleton R. 1990. Low ^{10}Be and ^{26}Al contents of ureilites: Production at meteoroid surfaces. *Geochim. Cosmochim. Acta* 54: 1775-1784.

Berkley J.L., Brown H.G., Keil K., Carter N.L. Mercier J-C.C. and Huss G. 1976. The Kenna ureilite: an ultramafic rock with evidence for igneous, metamorphic, and shock origin. *Geochim. Cosmochim. Acta* 40: 1429-1437.

Berkley J.L. 1989. Precision minor element analyses of silicate minerals in ureilites. *Lunar Planet. Sci. XX*: 61-62 (abstr.).

Borovicka J. and Charvat Z. 02009. Meteosat observation of the atmospheric entry of 2008 TC3 over Sudan and the associated dust cloud. *A & A* 507: 1015-1022.

Boynton W.V., Starzyk P.M. and Schmitt R.A. 1976. Chemical evidence for the genesis of the ureilites, the achondrite Chassigny and the nakhlites. *Geochim. Cosmochim. Acta* 40: 1439-1447.

Busemann H., Baur H. and Wieler R. 2000. Primordial noble gases in “phase Q” in carbonaceous and ordinary chondrites studied by closed-system stepped etching. *Meteorit. Planet. Sci.* 35: 949-973.

Clayton R.N. and Mayeda T.K. 1988. Formation of ureilites by nebular processes. *Geochim. Cosmochim. Acta* 52: 1313-1318.

Eugster O. and Michel Th. 1995. Common asteroid break-up events of eucrites, diogenites, and howardites and cosmic-ray production rates for noble gases in achondrites. *Geochim. Cosmochim. Acta* 59: 177-199.

Göbel R., Ott U. and Begemann F. 1978. On trapped noble gases in ureilites. *J. Geophys. Res.* 83: 855-867.

Goodrich C.A., Jones J.H. and Berkley J.L. 1987. Origin and evolution of the ureilite parent magmas: Multi-stage igneous activity on a large parent body. *Geochim. Cosmochim. Acta* 51: 2255-2273.

Goodrich, C.A. 1992. Ureilites: A critical review. *Meteoritics* 27: 327-352.

Grady M.M. and Pillinger C.T. 1988. ^{15}N-enriched nitrogen in polymict ureilites and its bearing on their formation. *Nature* 331: 321-323.

Heber V.S., Wieler R., Baur H., Olinger C., Friedmann T.A. and Burnett D.S. 2009. Noble gas composition of the solar wind as collected by the Genesis mission. *Geochim. Cosmochim. Acta* 73: 7414-7432.

Higuchi H., Morgan J.W., Ganapathy R. And Anders E. 1976. Chemical fractionations in meteorites, X, Ureilites. *Geochim. Cosmochim. Acta* 40: 1563-1571.

Jenniskens P., et al. 2009. The impact and recovery of asteroid 2008 TC_3. *Nature* 458: 485-488.

Koscheev, A.P., Gromov M.D., Mohapatra R.K. and Ott U. 2001. History of trace gases in presolar diamonds inferred from ion implantation experiments. *Nature* 412: 615-617.

Lee D.C., Halliday A.N., Singletary S.J. and Grove T.L. 2009. 182Hf-182W chronometry and early differentiation of the ureilite parent body. *Earth Planet. Sci. Lett.* 288: 611-618.

Matsuda J., Fukunaga K. and Ito K. 1991. Noble gas studies in vapor-growth diamonds: Comparison with shock-produced diamonds and the origin of diamonds in ureilites. *Geochim. Cosmochim. Acta* 55: 2011-2023.

Matsuda J. and Yoshida T. 2001. The plasma model for the origin of the phase Q: An experimental approach and the comparision with the labyrinth model. *Meteorit. Planet. Sci*. 36: A127 (abstr.).

Mittlefehldt D.W., McCoy T.J., Goodrich C.A. and Kracher A. 1998. Non-chondritic meteorites from asteroidal bodies. In: *Papike J.J. (Ed.), Planetary Materials. Mineralogical Society of America.* P 4-1-195.

Murty S.V.S. 1997. Noble gases and nitrogen in Muong Nong tektites. *Meteorit. Planet. Sci.* 32: 687-691.

Okazaki R., Nakamura T., Takaoka N. and Nagao K. 2003. Noble gases in ureilites released by crushing. *Meteoritics & Planetary Science* 38: 767-781.

Ott U., Löhr H.P. and Begemann F. 1984. Ureilites: the case of missing diamonds and a new neon component (abstract). *Meteoritics* 19: 287-288.

Ott U., Löhr H.P. and Begemann F. 1985. Trapped neon in ureilites – a new component. *In isotopic ratios in the solar system / Rapports isotopiques dans le systeme solaire*, pp. 129-136. Centre National d'Etudes Spatiales, Paris, 19-22 June 84/19-22 Juin 84.

Ott U., Löhr H.P. and Begemann F. 1993. Solar noble gases in polymict ureilites and an update on ureilite noble gas data. *Meteoritics* 28: 415-416 (abstr.).

Ott U., Hermann S., Jenniskens P.M. and Shaddad M. 2010. A noble gas study of two stones from the Almahata Sitta meteorite. Lunar Planet. Sci. Conf. 1195.pdf

Ozima M. 1989. Gases in diamonds. *Ann. Rev. Earth Planet. Sci.* 17: 361-384.

Ozima M., Wieler R., Marti B. and Podosek F.A. 1998. Comparative study of solar, Q-gases and terrestrial noble gases, and implications on the evolution of the solar nebula. *Geochim. Cosmochim. Acta* 62: 301-314.

Ozima M. And Podosek F.A. 2002. Noble gas geochemistry, 2nd edition. Cambridge Univ. Press, Cambridge.

Rai V.K., Murty S.V.S. and Ott U. 2002. Nitrogen in diamond-free ureilite Allan Hills 78019: Clues to the origin of diamond in ureilites. *Meteorit. Planet. Sci.* 37: 1045-1055.

Rai V.K., Murty S.V.S. and Ott U. 2003a. Noble gases in ureilites: Cosmogenic, radiogenic, and trapped components. *Geochim. Cosmochim. Acta* 67, 4435-4456.

Rai V.K., Murty S.V.S. and Ott U. 2003b. Nitrogen components in ureilites. *Geochim. Cosmochim. Acta* 67: 2213-2237.

Ross A., Steele A., Downes H., Fries M., Jenniskens P., Jones A., Kater L., Smith C., Zolensky M. 2010. MicroRaman spectroscopy of diamond in Almahata Sitta and comparisons with other ureilites. Submitted to *MAPS*.

Scott E.R.D., Taylor G. and Keil K. 1993. Origin of ureilite meteorites and implications for planetary accretion. *Geophys. Res. Lett.* 20: 415-418.

Singletary S.J. and Grove T.L. 2003. Early petrologic processes on the ureilite parent body. *Meteoritics & Planet Science* 38: 95-108.

Spitz A. H. and Boynton W.V. 1991. Trace element analysis of ureilites: New constraints on their petrogenesis. *Geochim. Cosmochim. Acta* 55: 3417-3430.

Takeda H. 1987. Mineralogy of Antarctic ureilites and a working hypothesis for their origin and evolution. *Earth Planet. Sci. Lett.* 81: 358-370.

Takeda H., Mori H. And Otaga H. 1989. Mineralogy of augite-bearing ureilites and the origin of their chemical trends. *Meteoritics* 24: 73-81.

Vdovykin G.P. 1976. The Haverö meteorite. *Space Sci. Rev.* 18: 749-776.

Wacker J.F. 1986. Noble gases in the diamond-free ureilite, ALH78019: The roles of shock and nebular processes. *Geochim. Cosmochim. Acta* 50: 633-642.

Wacker J.F. 1989. Laboratory simulation of meteoritic noble gases. III. Sorption of neon, argon, krypton and xenon on carbon: Elemental fractionation. *Geochim. Cosmochim. Acta* 53: 1421-1433.

Walker D. And Grove T.L. 1993. Ureilite smelting. *Meteoritics* 28: 629-636.

Warren P.H and Kallemeyn G.W. 1989. Geochemistry of polymict ureilite EET83309, and a partially-disruptive impact model for ureilite origin. *Meteoritics* 24: 233-246.

Warren P.H and Kallemeyn G.W. 1992. Explosive volcanism and graphite-oxygen fugacity buffer on the parent asteroid(s) of ureilite meteorites. *Icarus* 100: 110—126.

Wasson J.T., Chou C.-L., Bild R.W. and Baedecker P.A. 1976. Classification of and elemental fractionation among ureilites. *Geochim. Cosmochim. Acta* 40: 1449-1458.

Welten K.C., Meier M.M.M., Caffee M.W., Nishiizumi K., Wieler R., Jenniskens P. and Shadad M.H. 2010. Cosmogenic nuclides in Almahata Sitta ureilite: Cosmic ray exposure age, pre-atmospheric mass and bulk density of asteroid 2008 TC_3. *Meteoritics Planet Sci.(This issue)*

Wilkening L.L. and Marti K. 1976. Rare gases and fossil tracks in the Kenna ureilite. *Geochim. Cosmochim. Acta* 40: 1465-1473.

Yamamoto T., Hashizume K., Matsuda J.I. and Kase T. 1998. Multiple nitrogen components coexisting in ureilites. *Meteoritics Planet Sci.* 33: 857-870.

Yeomans D. 2008. NASA/JPL Near-Earth Object Program Office Statement (http://neo.jpl.nasa.gov/news/news159.html) (6 October, 2008).

Ziegler J.F., Biersack J.P. and Littmark U. 1985. The Stopping Range of Ions in Solids. Permagon Press, Tarrytown, N. Y., 321pp.

Zolensky M. et al. 2010. Mineralogy and petrology of the Almahata Sitta ureilite. *Meteoritics Planet Sci.(This issue)*

FIGURE CAPTIONS

Fig. 1. SEM pictures of the HF/HCl resistant residue of Almahata Sitta. Most of the residue is a cluster of crystalline structures. EDX spectra of most crystals shows only C peak. Graphite (G) with layered structure (dark grey) and whitish crystals of Diamond (D) of few microns to sub-micron sizes are seen in all the four pictures. Amorphous carbon, seen as a fine coating on the dark grey graphites, seems to be low in abundance.

Fig. 2. Ne three isotope plot for the bulk sample of AS. Cosmogenic (Göbel et al., 1978), SW (Heber et al., 2009), Ne-U (Ott et al., 1985) and Air (Ozima and Podosek, 2002) values are also indicated.

Fig. 3. Release pattern of ^{3}He is shown along with C release (monitored as CO + CO_2 pressure) for the bulk and residue samples of AS.

Fig. 4. Release patterns of C (monitored as CO + CO_2 pressure), N and δ^{15}N (upper panels) and Ar, Kr and Xe (lower panels) for the bulk and the residue samples of AS.

Fig. 5. Release patterns of C (monitored as CO + CO_2 pressure), N, Ar, Kr and Xe for the residue sample of AS are compared with those from ALH 78019 (diamond free ureilite), LEW 85328 (typical monomict ureilite), EET 87720 (typical polymict ureilite) and ALH 82130 (low shocked ureilite showing Xe enrichment), data for which is taken from Rai et al., (2003a).

Fig. 6. Elemental ratios $^{36}Ar/^{132}Xe$ and $^{84}Kr/^{132}Xe$ at different extraction temperatures for the bulk and residue of AS are compared.

Fig. 7. The elemental ratios $^{132}Xe/^{36}Ar$ and $^{84}Kr/^{36}Ar$ are plotted againt each other. These ratios vary by more than two orders of magnitude among ureilites, but normally fall along the mass fractionation trend (shown as the line MFL, taken from Fig. 12 of Rai et al., 2003a). The data of AS residue falls close to MFL, while the data for AS bulk falls much above the MFL line, indicating excess ^{132}Xe in AS bulk. Similar Xe excess has been earlier observed in case of ureilite ALH82130 [data shown are from Ott et al., 1986 (for A30-B2) and Rai et al., 2003a (for A30-B1, A30-Res)].

Fig. 8. The variation of the isotopic ratio $^{38}Ar/^{36}Ar$ with extraction temperature is shown for the residue sample of AS. The amount of ^{36}Ar released in each temperature fraction is also shown. Average value of $^{38}Ar/^{36}Ar$ for ureilite residues (Göbel et al., 1978) and the value for the total of AS residue are also shown.

Fig. 9. $^{38}Ar/^{36}Ar$ vs. $\delta^{15}N$ for the individual temperature steps of AS residue. The low temperature (LT) and high temperature (HT) data cluster into two fields, indicating the presence of two different components.

Table 1. Noble gas abundances and isotopic ratios for the totals in the bulk sample (AS#36) and HF/HCl residue (prepared from AS#44) of Almahata Sitta. Abundances are in ccSTP/g units. Errors in isotopic ratios are at 95% confidence limits. Errors in concentrations are ±10% (for He, Ne, Ar) and ±15% (for Kr and Xe).

Sample (wt. mg)	^{4}He 10^{-6}	^{22}Ne 10^{-6}	^{36}Ar 10^{-6}	^{3}He/^{4}He (10^{-4})	^{20}Ne/^{22}Ne	^{21}Ne/^{22}Ne	^{38}Ar/^{36}Ar	^{40}Ar/^{36}Ar	^{84}Kr 10^{-10}	^{132}Xe 10^{-10}
Bulk (30.62)	13.0	0.123	0.435	178.6 ±15.1	2.986 0.092	0.7360 0.0116	0.1954 0.0003	6.810 0.043	32.34	102.3
Residue (1.23)	682	1.23	453.3	-	-	-	0.1908 0.0002	0.2058 0.0011	17106	12211

Table 2. Nitrogen, trapped and cosmogenic noble gas amounts in AS samples. Production rates P3 and P21 are in units of 10^{-10} ccSTP/g/Ma units (for details of calculation, see text).

Errors in N are ±10% and errors in $\delta^{15}N$ correspond to 95%CL. The trapped gas amounts are normalised to ^{132}Xe. Errors in cosmic ray exposure ages (T_3 and T_{21}) are ±15%

Samples	N ppm	$\delta^{15}N$ ‰	$^{3}He_c$ 10^{-8}	$^{21}Ne_c$ 10^{-8}	P_3	P_{21}	T_3 Ma	T_{21} Ma	Ratios ($^{i}X/^{132}Xe$) ^{4}He	^{20}Ne	^{36}Ar	^{84}Kr	^{132}Xe
Bulk	21.1	-36.80 ±0.78	23.2	9.08	167.9	56.7	13.8	16.0	1268	27.1	42.5	0.316	≡1.00
Residue	249.5	-74.3 0.61	12.6	-			-	-	558	11.5	371	1.401	≡1.00

Table 3. Data for temperature fractions of bulk and HF/HCl residue of Almahata Sitta samples. Data for the totals are listed in Table 1. P* indicates pyrolysis, while at other temperatures, it is combustion. **C release has been monitored as the evolved (CO + CO_2). #For the residue sample only ^{3}He concentrations are listed under the column (^{3}He/^{4}He), in 10^{-8} ccSTP/g units.

Temp. (°C)	^{4}He 10^{-6}	^{22}Ne 10^{-8}	^{36}Ar 10^{-6}	^{3}He/^{4}He 10^{-4}	N ppm	δ^{15}N ‰	^{20}Ne/^{22}Ne	^{21}Ne/^{22}Ne	^{38}Ar/^{36}Ar	^{40}Ar/^{36}Ar	^{14}N/^{36}Ar 10^3	^{84}Kr/^{36}Ar 10^{-3}	^{132}Xe/^{36}Ar 10^{-3}	C Release** %
Bulk Sample #36 (30.62 mg)														
300	1.09	0.447	0.005	124.1 ±10.5	2.77	24.4 0.8	9.511 0.178	0.0728 0.0009	0.1951 0.0002	39.1 0.1	886	18.0	36.4	~0
400	0.78	0.393	0.005	272.4 23.1	1.82	31.8 0.5	9.998 0.169	0.0952 0.0013	0.2008 0.0009	40.8 0.5	598	13.1	41.8	~0
600	1.90	0.554	0.024	181.6 15.4	1.80	27.7 0.9	8.964 0.150	0.1660 0.0027	0.1919 0.0009	25.9 0.1	118.3	9.9	51.8	~0
800	4.56	1.043	0.096	107.1 9.1	3.27	-65.3 0.5	6.731 0.267	0.4319 0.0179	0.1893 0.0005	7.78 0.01	54.2	9.2	44.8	27.8
1000	2.01	1.26	0.156	173.3 14.7	6.15	-94.3 0.8	4.040 0.207	0.6019 0.0230	0.1893 0.0001	4.38 0.05	63.2	5.7	15.5	42.8
1200P*	0.56	1.68	0.058	917.9 77.7	3.89	-23.1 0.8	1.771 0.050	0.8359 0.0112	0.2008 0.0009	4.45 0.03	106.4	5.3	10.0	7.4
1400P*	1.42	3.22	0.078	175.9 14.9	0.821	-69.4 2.4	1.162 0.045	0.9667 0.0137	0.2074 0.0001	2.41 0.01	16.8	8.0	14.8	12.2
1800P*	6.51	3.67	0.011	36.5 3.1	0.573	-20.4 0.5	1.094 0.031	0.8895 0.0091	0.2273 0.0002	4.12 0.19	80.7	10.4	8.9	9.8

HF/HCl Residue from #44 (1.23 mg)														
300	81.0	16.97	2.80	~0[#]	16.61	8.74 0.24			0.1890 0.0002	1.185 0.008	9.5	3.05	2.23	~0
400	67.9	12.26	5.45	0.95[#]	23.95	12.0 0.6			0.1891 0.0002	0.3540 0.0031	7.0	3.32	2.46	~0
450	46.0	12.37	6.30	0.69[#]	18.33	8.82 0.87			0.1896 0.0001	0.1906 0.0039	4.65	3.46	2.76	~0
500	24.9	7.33	23.4	1.06[#]	14.95	4.62 0.46			0.1905 0.0002	0.6197 0.0084	1.02	3.24	2.97	2.3
600	165.9	24.99	105.3	3.00[#]	32.23	-96.0 1.2			0.1902 0.0005	0.1815 0.0011	0.49	2.96	2.26	21.0
700	138.8	22.47	164.5	1.85[#]	77.42	-115.3 0.1			0.1910 0.0001	0.1412 0.0002	0.75	2.19	2.79	39.0
800	80.8	16.43	78.0	1.93[#]	49.14	-106.8 0.8			0.1910 0.0001	0.1969 0.0012	1.0	4.31	2.78	15.6
1030	76.4	10.62	67.5	3.16[#]	16.92	-114.4 1.1			0.1916 0.0001	0.2165 0.0003	0.4	5.14	2.98	21.9

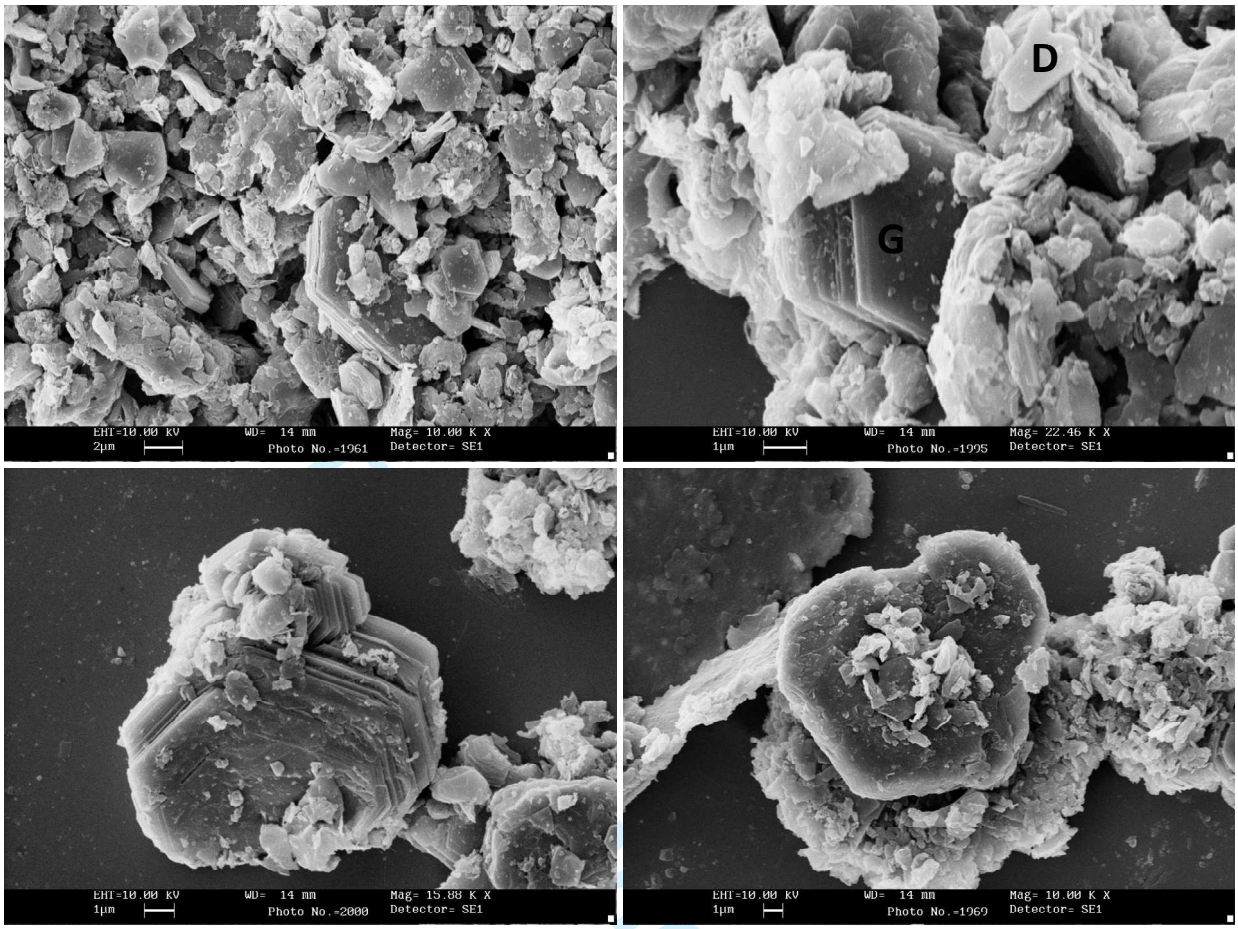

Fig. 1 (Murty et al., 2010, MAPS)

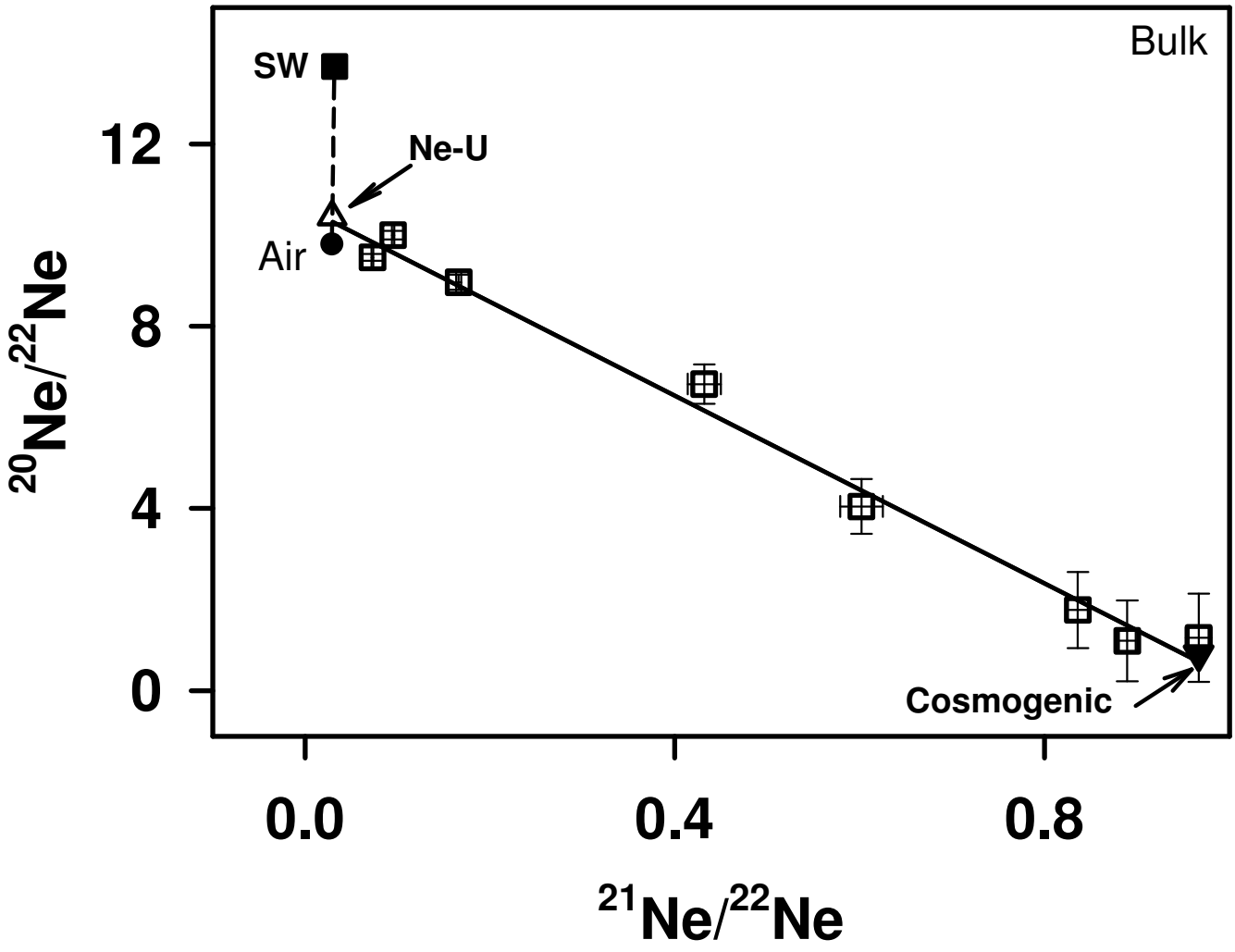

Fig. 2 (Murty et al., 2010, MAPS)

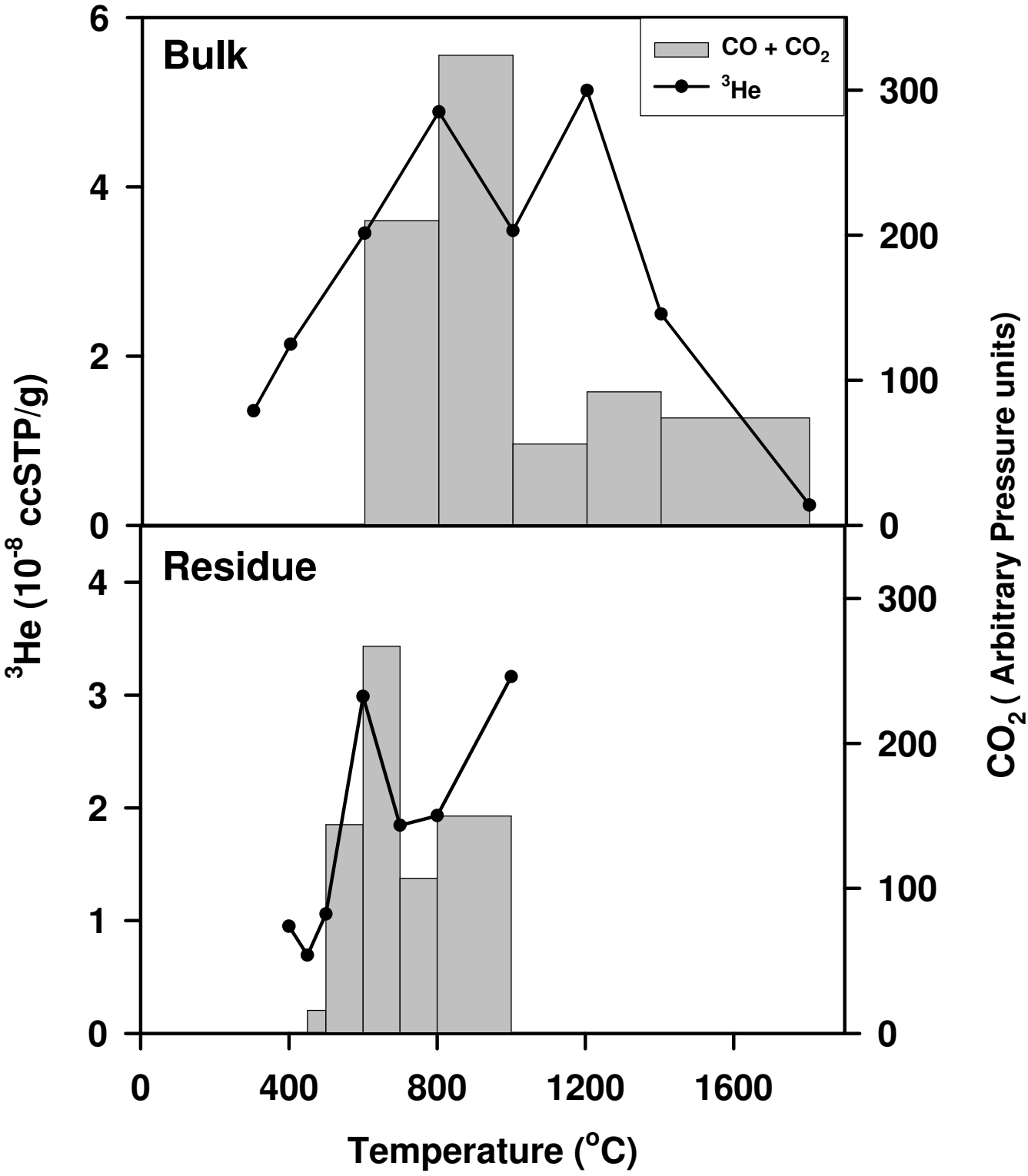

Fig. 3 (Murty et al., 2010, MAPS)

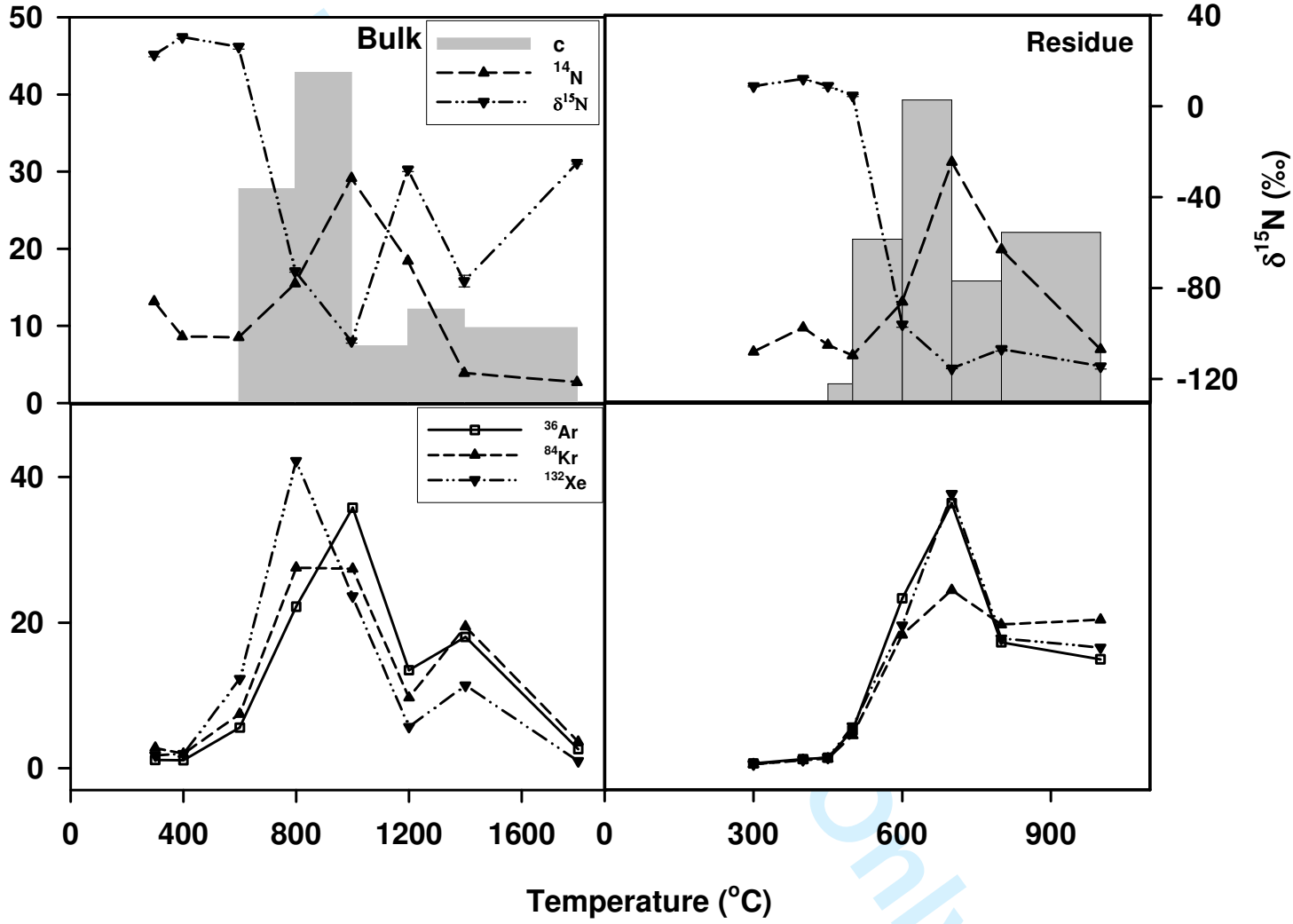

Fig. 4 (Murty et al., 2010, MAPS)

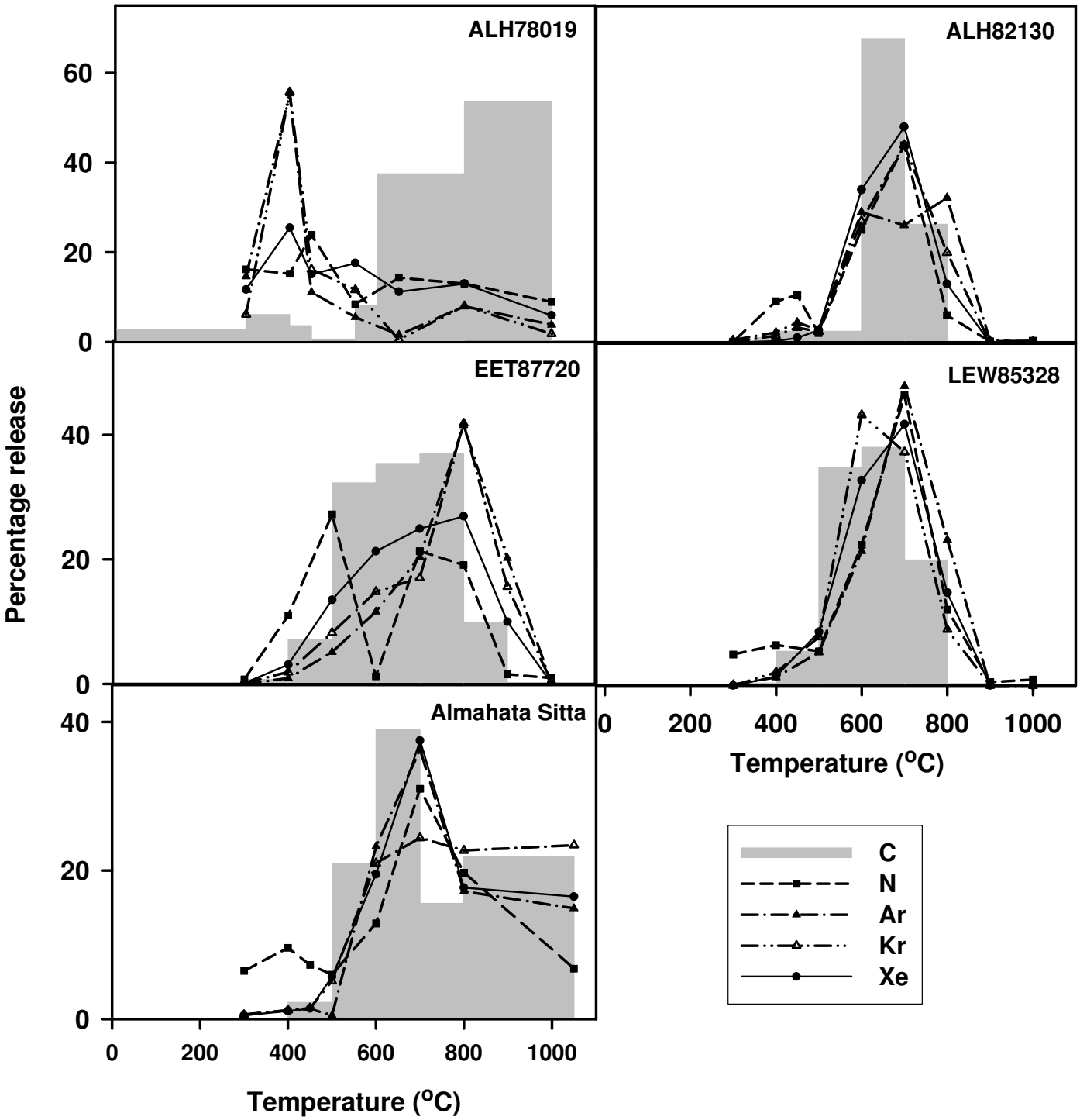

Fig. 5 (Murty et al., 2010, MAPS)

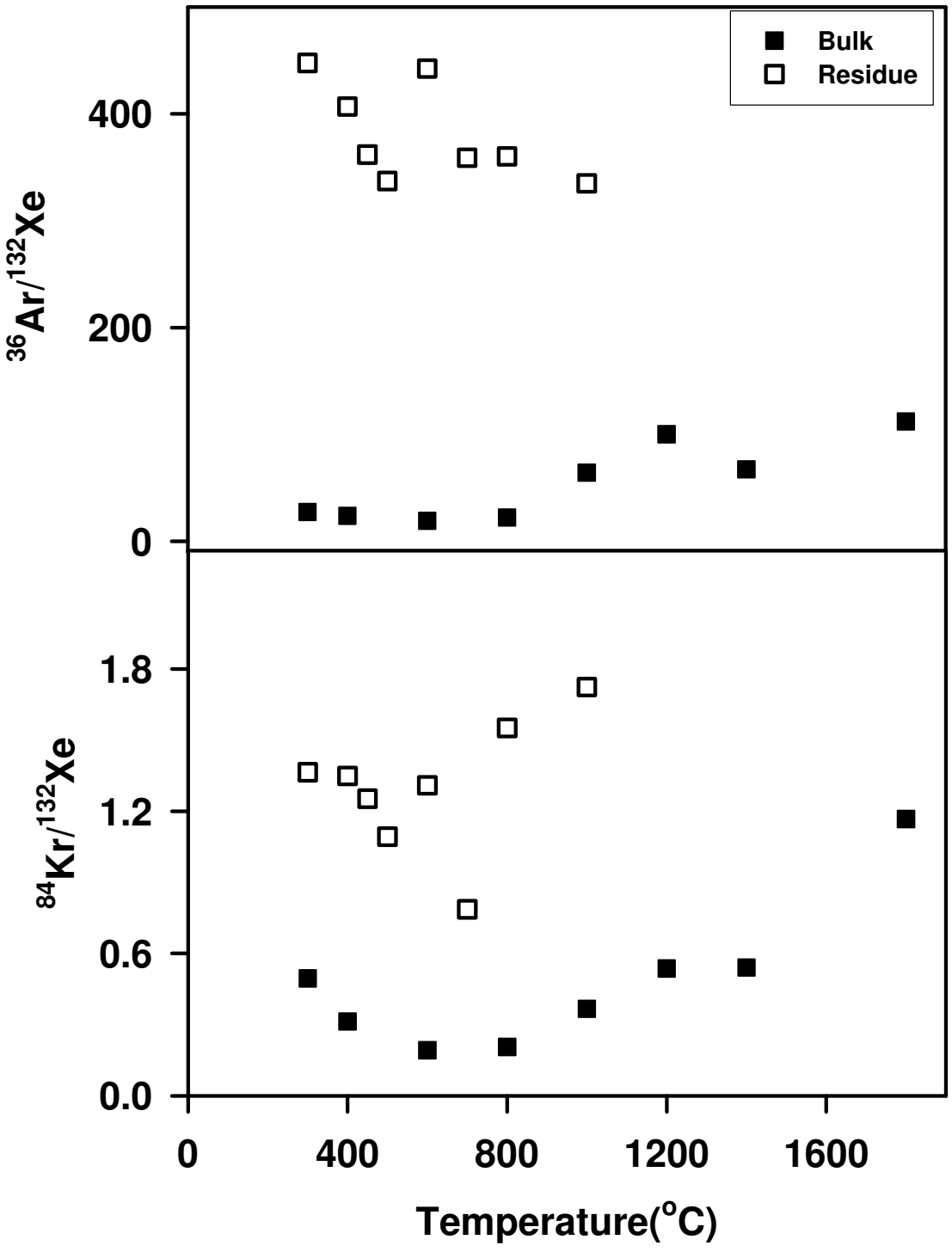

Fig. 6 (Murty et al., 2010, MAPS)

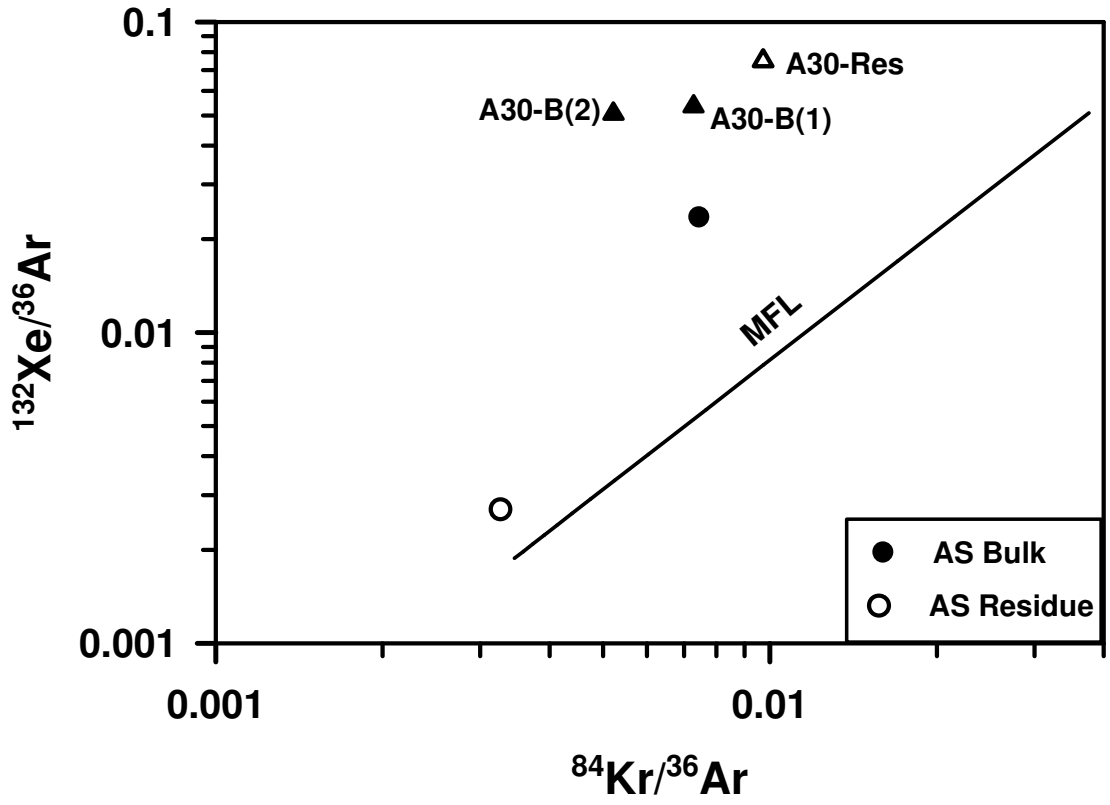

Fig. 7 (Murty et al., 2010, MAPS)

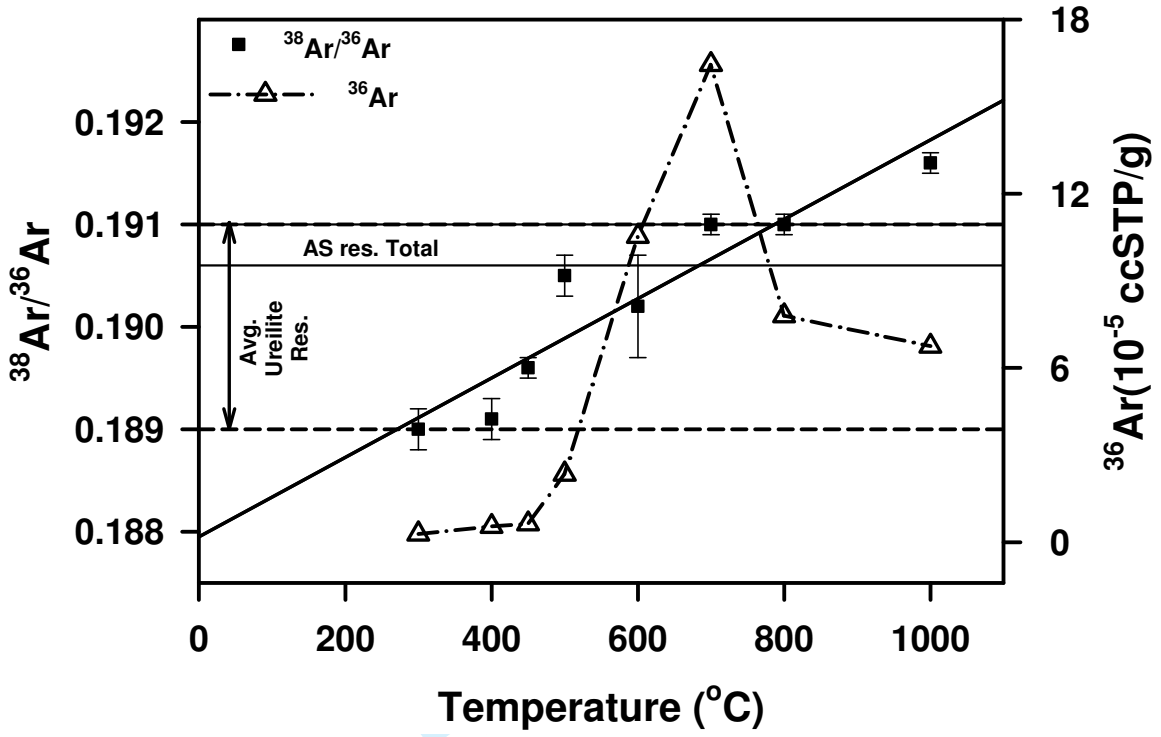

Fig. 8 (Murty et al., 2010, MAPS)

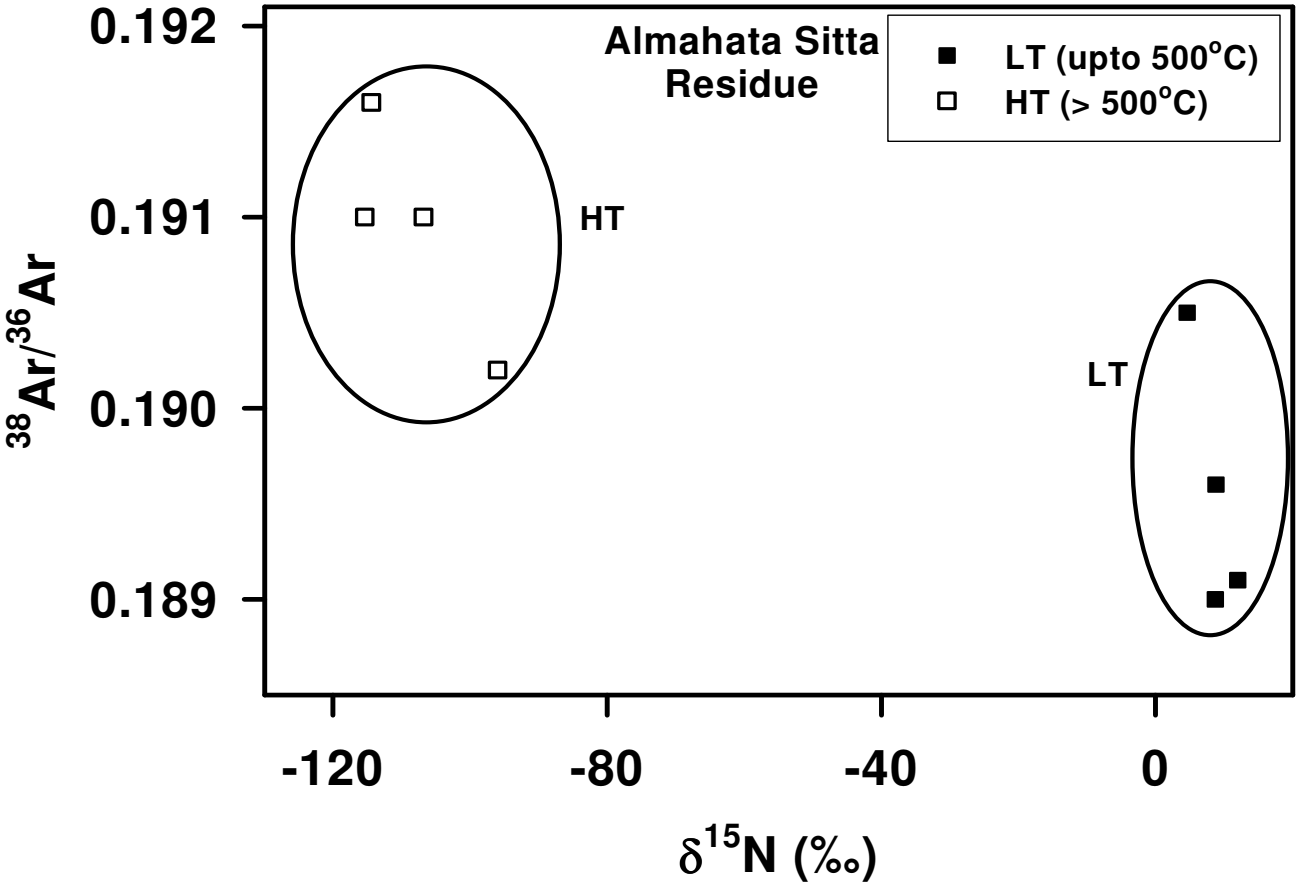

Fig. 9 (Murty et al., 20010, MAPS)